Characteristics of carbonate, evaporite and silicate weathering in Huanghe River basin: A comparison among the upstream, midstream and downstream

Bai-Ling Fan [a,b], Zhi-Qi Zhao [a,*], Fa-Xiang Tao [a], Bao-Jian Liu [a,b,c], Zheng-Hua Tao [a,b], Shuang Gao [a,b], Li-Hua Zhang [a]

[a] State Key Laboratory of Environmental Geochemistry, Institute of Geochemistry, Chinese Academy of Sciences, Guiyang 550002, China
[b] University of Chinese Academy of Sciences, Beijing 100049, China
[c] State Key Laboratory of Organic Geochemistry, Guangzhou Institute of Geochemistry, Chinese Academy of Sciences, Guangzhou 510640, China

ARTICLE INFO

ABSTRACT

To systematically study chemical weathering in the entire Huanghe River basin, we divided the basin into three parts with significant differences in geology and climate. We collected 38 water samples from the main channel and its main tributaries, spread between the upstream (above Lanzhou), midstream (from Lanzhou to Huayuankou) and downstream (from Huayuankou up to river mouth) segments of the river. The concentrations of major elements and H, O isotopic compositions were obtained from the samples, and the total dissolved solids (TDS) and, CO_2 consumption budget were calculated from the aggregated data of each of the three segments. The results demonstrate that: the TDS are mainly derived from carbonate weathering in upper Huanghe River; evaporite dissolution is predominately occurred in the midstream; and there is almost no additional contribution from rock weathering in the downstream. An increasing trend of CO_2 consumption rate by silicate weathering is observed, from 0.14×10^5 mol/km^2/yr in the upstream to 5.62×10^5 mol/km^2/yr in the downstream, and the budget of CO_2 consumption by silicate weathering is estimated to be 26.2×10^9 mol/yr. In contrast, the CO_2 consumption rate by carbonate weathering decreases from 3.04×10^5 mol/km^2/yr in the upstream to near zero in the downstream, and the budget of CO_2 consumption is estimated to be 100.5×10^9 mol/yr. As a whole, in the entire Huanghe River basin, the CO_2 consumption budget and TDS yield are estimated to be 126.7×10^9 mol/yr, and 27.5×10^6 t/yr, respectively. These results indicate that evaporite dissolution in the midstream is responsible for the high TDS in the Huanghe River basin, while carbonate weathering in the upstream plays the most significant role in CO_2 consumption.

1. Introduction

Continental weathering is thought to play an important role in the long-term carbon cycle, and thus to regulate global climate on geological time scales through consumption of atmospheric CO_2 (Berner et al., 1983; Dessert et al., 2003; Gaillardet et al., 1995; Meybeck, 1987; Raymo et al., 1988). Weathering is also a key process controlling the geochemical cycle of elements, because many elements are released in abundance during rock weathering (Gaillardet et al., 1995; Gardner et al., 1981; Gibbs, 1972; Huh et al., 1998; Zhang et al., 1995). Silicate, carbonate and evaporite rocks weather differently and each displays a different role in

carbon cycles and riverine chemical compositions. During silicate weathering, which is accompanied by CO_2 consumption and thought to be the dominant long-term sink of atmosphere CO_2, primary minerals are decomposed and then converted to residue clays, dissolved loads, and silica. Carbonate weathering is not accompanied by secondary mineral formation, and has an effect on the CO_2 cycle only on a short time scale, though the dissolution rate of carbonate is thought to be much faster than that of silicate. However, carbonate weathering is considered to be more important than the weathering of silicate minerals in controlling river water chemistry (Fairchild et al., 1994; Han and Liu, 2004). The dissolution of evaporite minerals does not consume CO_2, but it does exert an important role in chemical composition of river waters, even if evaporite outcrops are rather rare in the watershed (Meybeck, 1987; Ryu et al., 2008), because evaporite is more

susceptible to weathering compared with silicate and carbonate, and such dissolution can generate K, Na, Ca, Mg, Cl and SO$_4$.

Rivers carry the products of chemical weathering in dissolved phases or in solid form, and transport these products seaward. Rivers, particularly large rivers, are of great importance for substance circulation. The 30 largest rivers of the world are thought to represent half of the total runoff to the ocean (Gaillardet et al., 1999). To gather the fundamental information about the evolution of the Earth's surface, geologists have paid much attention to large rivers (Chetelat et al., 2009, 2008; Gaillardet et al., 1995, 1999; Galy et al., 1999). For instance, one of the world's largest rivers, the Amazon River, has been investigated since 1903 (Gaillardet et al., 1997; Gibbs, 1972). Generally, the geochemical investigation of large rivers allows us to obtain important information about weathering processes, matter cycles in the continent–river–ocean system, and CO$_2$ consumption associated with the weathering of continental rocks. In an extremely large watershed the lithology of the drainage basin is complex, and it is important to distinguish the sources of geochemical weathering along different reaches of the river system.

The Huanghe River (Yellow River), one of the world's largest rivers, transports approximately 14.8×10^9 m^3/yr of water and about 2.88×10^{11} kg/yr of suspended sediment, on average, to seaward (1987–2010 data from http://www.yellowriver.gov.cn/nishagonggao/2012/index, in Chinese). It accounted for a large part of the world sediment load input to ocean, and the River is the most important water source for northern China, so it has received significant attention from geologists since the 1980s (Wang et al., 2012, 2006; Wu et al., 2005; Zhang et al., 1995, 1990a). However, most of previous research on chemical weathering in the Huanghe River basin was based on samples near its mouth (Wang et al., 2012) or near its headwater (Wu et al., 2005), with few studies based on sampling throughout the whole basin (Zhang and Wen, 2009). As a result, the knowledge of chemical weathering in the entire Huanghe River basin is limited.

For his study, we used a synoptic-sampling approach to examine the qualitative and quantitative estimations of the TDS yield and CO$_2$ flux from the contribution of silicate, carbonate and evaporite weathering in the upstream, midstream and downstream of the Huanghe River. In particular, we aimed to characterize the aqueous geochemistry and its controlling factor(s) along different reaches of the river, and to get a clear understanding of the role of the three kinds of rock in the basin.

2. Geography, climate and lithology of the drainage catchments

The Huanghe River (basin surface area = 752,000 km^2) located in northwestern China, flows from its source in high mountainous areas in the northeast of Tibet at about 5000 m elevation to its outlet into the Bohai Sea (Fig. 1). The basin displays complex features in lithology and topography, covered all kinds of rocks from Cambrian to Quaternary period. The source areas of the Huanghe River, from Lanzhou city upward with elevation of 2000–4000 m, is mainly comprised of detrital rocks of late Palaeozoic age to Mesozoic age, including coal bearing formations and red-beds, and limestones. The midstream segment of the river (from Lanzhou to Huayuankou) drains the Loess Plateau, which accounts for 44% of the total watershed area. Erosion on the Loess Plateau leads to extremely high sediment yield, and a large amount of unconsolidated sediment spread downstream (Saito et al., 2001; Wu et al., 2005; Zhang et al., 1995).

Except for the source area, which is characterized by high elevation and cold climate, the main body of the Huanghe River basin is subjected to a warm climate, with mean annual temperature of 1–8 °C in the upstream segment, 8–14 °C in the midstream

segment, and 12–14 °C in the downstream segment. Mean annual rainfall in the watershed is 476 mm, and is unevenly distributed, increasing from 150 mm for upstream and midstream to 900 mm for downstream. The Huanghe River basin also suffers strong surface evaporation of about 1100 mm annually (Chen and Wang, 2006; Zhang and Wen, 2009).

3. Materials and analytical methods

3.1. Sampling

Samples were collected from the Huanghe River, divided among its three main parts: upstream (above Lanzhou, samples MH01, MH02, M1–M5), midstream (from Lanzhou to Huayuankou, samples M6–M19 and downstream (Huayuankou to Dongying, samples M20–M23). These divisions were based on differences in the geologic and climatic factors. Samples were collected in August 2012 along the Huanghe River main channel and its main tributaries (Fig. 1). Between 15 and 20 L of river water was collected and filtered within a few hours after collection through 0.45 μm cellulose acetate filters. The first liter was discarded and the following liters were stored in acid-washed polyethylene bottles, for analysis after acidification to pH-2 with double-distilled HCl. Two aliquots were prepared: one acidified for cations analysis, and another non-acidified for the anions determination.

3.2. Analytical methods

The temperature, pH and electric conductivity (EC) were measured in field. Alkalinity was determined with the Gran titrating method using 0.02 M HCl. Concentrations of cations and anions for the water samples were determined in the State Key Laboratory of Environmental Geochemistry using ICP-OES and Ion Chromatography with uncertainties of 5% and 8%, respectively.

Stable δ^{18}O and δD were determined by Liquid–Water Isotope Analyzer in the State Key Laboratory of Environmental Geochemistry. The precision of chemical analyses was estimated through repeated determinations of standards. The external precision for δ^{18}O and δD were 0.07‰ and 0.12‰, respectively.

4. Results

4.1. Hydrogeochemistry

Hydrological parameters (pH, T and EC), concentrations of major elements and O, H isotope compositions of the water samples are presented in Table 1. The pH of river water samples range from 7.42 to 9.82, with a mean value of 8.02. The highest pH values are observed for a headwater tributary (MH02, pH = 9.82) and a tributary in the mainstream (T4, pH = 9.48). The EC values vary from 0.6 to 11,440 μS/cm. The water temperature generally increase from upstream (9.6 °C, M2) to downstream (29.1 °C, M18) along the Huanghe River main channel, controlled by the progression to lower elevation and warmer climate of the sampling sites. The total cationic concentrations (in meq/L, TZ$^+$ = Na$^+$ + K$^+$ + 2Mg^{2+} + 2Ca^{2+}) for most water samples range from 3 to 10 meq/L, except for five samples with much higher values (11–151 meq/L) in the tributaries. TZ$^+$ is much higher than the average value of the world's rivers (1.25 meq/L, Meybeck, 1981). The total dissolved cations are mostly balanced with the total dissolved anions (TZ$^-$ = Cl$^-$ + 2SO$_4^{2-}$ + HCO$_3^-$) within 5%. Compared with the world's major rivers (Gaillardet et al., 1999), the Huanghe River samples have the highest values in terms of TDS, varying from 261.5 to 9177 mg/L, with an average of 557 mg/L. The
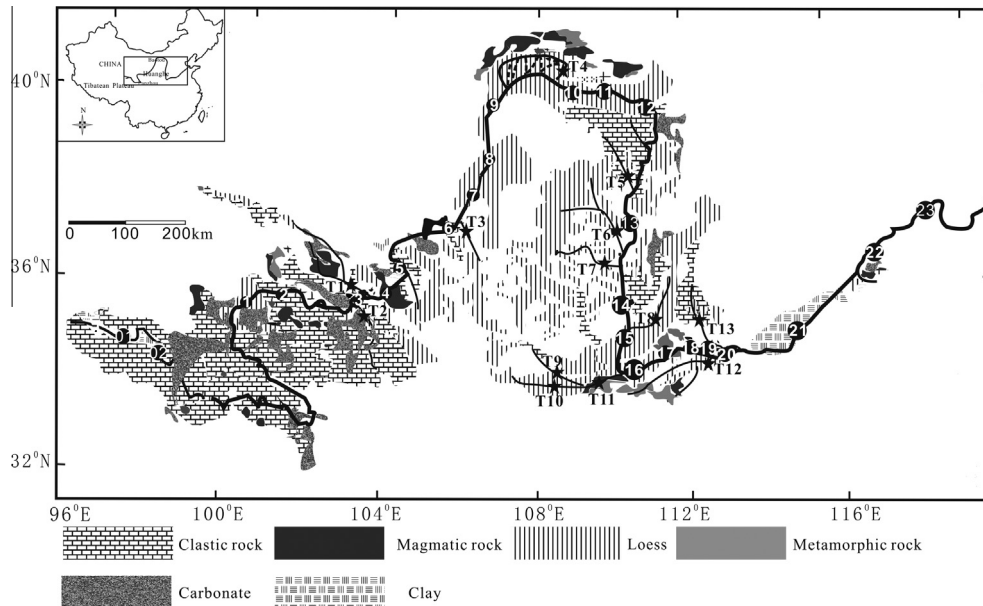
Fig. 1. Map showing geology, sampling sites, and river flow in the Huanghe River basin. The numbers in the circle represent headwater and main channel river samples in the Huanghe River basin.

headwater tributary (site MH02) and two tributaries (sites T3, T4) exhibit extremely high TDS.

4.2. Major ions distribution

Variations of dissolved major elements in the Huanghe River water are compared with some other large rivers in Fig. 2. The water chemical composition differ significantly between the upstream and the midstream of the Huanghe River, while the difference between midstream and downstream is unclear. The major elemental composition in tributaries is highly variable. For the Huanghe River main channel, the chemical composition change from $Ca + HCO_3$ in the upstream samples to $Na + Cl + SO_4$ in the downstream areas. Cationic composition of upstream samples are mostly dominated by Ca with an order of Ca > Na > Mg > K, except for two Na-dominant samples (sites MH01, MH02) taken from headwater tributaries. Sodium is the dominant cation in the midstream and downstream, with Na > Ca > Mg > K. Bicarbonate (HCO_3) is the dominant anion for all water samples, accounting for 70% of the TZ^- in the upstream samples, 54% for the midstream, 49% for the downstream. Cl and SO_4 are also important anions, accounting for over 40% of the anions for most of the samples. In general, there is an increasing trend in Cl and SO_4 concentrations from upstream to midstream.

The NO_3 concentrations range from 41 to 1828 μM in the whole basin and increase from the upstream (41 μM, site M1) to the downstream (238 μM, site M20) along the main channel. The highest concentration is observed in the tributary Qingshui River.

The dissolved Si concentrations vary between 23.7 and 441 μM and the highest concentrations are observed mostly in the downstream. Silicon increase from the upstream average of 146 μM, to the downstream, average of 300 μM, along the Huanghe River main channel.

4.3. $\delta^{18}O$ of river waters

The $\delta^{18}O$ values for most of the Huanghe River water samples range from −13.0‰ to −7.0‰, which is similar to previously reported values (Zhang et al., 1995), with the exception of three samples (site MH01 is −3.9‰, site MH02 is −3.3‰, and site T4 is −1.4‰). As shown in Fig. 3, these three samples clearly deviate from the global meteoric water line, probably because of the high level of evaporation occurring in these areas. The tributary (site T5) exhibits the lowest value, −13.7‰, which is similar to that of rain water sampled in Baotou −14.5‰. In general, there is an increasing trend for $\delta^{18}O$ from Lanzhou to Inner Mongolia Autonomous Region (M4−M10). As the river flows through Shaanxi and Shanxi Provinces, the $\delta^{18}O$ values decrease markedly. In the downstream, however, the $\delta^{18}O$ values increase again (Table 1).

5. Discussion

5.1. Sources of dissolved load

5.1.1. Atmospheric supply

Contribution of atmospheric input is typically considered to enhance chemical composition of riverine water. In some rivers, such as those influenced by evaporation, atmospheric input is substantially important, accounting for 70% of total TDS (Gaillardet et al., 1999). Cl is the most commonly used element to evaluate the atmospheric contribution to the chemical composition of river waters (Liu et al., 2013; Negrel et al., 1993; Stallard and Edmond, 1981), because its content is generally very low in carbonate and silicate rock. In pristine areas, Cl is entirely derived from the atmosphere, and by using the Cl normalized elemental ratios the concentrations of other elements can be corrected (Negrel et al., 1993). In the case of Huanghe River, however, the use of Cl as an index is not suitable because of the widespread evaporites in the upstream and midstream segment. Rather, F has successfully been used as an indicator to correct the atmospheric contribution to the dissolved load of rivers located in Changjiang basin (Chetelat et al., 2008).

As shown in Table 1, the F concentrations of the Huanghe River water samples range from 2.0 to 29.7 μM, and though they increase from the upstream to the downstream, they remain within the concentration range (from 1 to 35 μM) of precipitation samples (Larssen et al., 1999). Assuming that the chemical composition of rainwater for the entire watershed was constant, and using the F/element ratio for the rainwater in Qinghai (Zhang

Table 1
Chemical and D, O isotopic compositions of river waters in the main channel and major tributaries of the Huanghe River.

Sample	Location	pH	T (°C)	EC (µs cm⁻¹)	K⁺ (µM)	Na⁺ (µM)	Ca²⁺ (µM)	Mg²⁺ (µM)	Si (µM)	Cl⁻ (µM)	SO₄²⁻ (µM)	HCO₃⁻ (mM)	NO₃⁻ (µM)	F⁻ (µM)	TDS (mg/L)	δD (‰)	δ¹⁸O (‰)	NIBC*
Upstream																		
MH01	Lake Zhaling	8.70	10.7	0.6	58	1914	846	993	31	1738	229	3.77	0.00	6.9	422.1	−38.6	−3.9	−5.53
MH02	Maduo	9.82	10.5	2414.0	153	13,384	207	5753	24	14,187	1508	8.60	0.00	13.2	1643.2	−35.4	−3.3	−1.36
M1	Tangnaihai	7.82	14.0	301.8	30	252	1034	663	213	151	256	2.60	40.85	2.4	281.8	−76.2	−10.9	10.12
M2	Guide	8.22	9.6	413.8	37	597	1280	696	197	380	352	3.43	50.57	2.0	367.5	−78.2	−10.6	0.42
M3	Lanzhou	7.44	21.8	430.8	39	791	1313	710	174	477	538	3.17	58.67	4.9	376.4	−74.3	−10.2	2.02
M4	Lanzhou	8.09	17.6	467.7	42	919	1372	724	195	604	557	3.36	83.98	5.5	404.4	−62.9	−9.2	−0.07
M5	Lanzhou	8.11	20.1	473.1	43	943	1383	728	190	628	571	3.40	80.35	8.1	409.4	−68.6	−9.6	−0.82
Midstream																		
M6	Zhongwei	8.30	19.8	518.9	45	1193	1368	780	196	844	665	3.21	–	4.0	417.1	−67.9	−9.6	2.70
M7	Yingchuan	7.86	25.7	679.9	56	2198	1490	1007	202	1566	1044	3.68	–	7.5	542.4	−67.4	−9.4	−1.14
M8	Wuhai	7.71	22.9	1004.0	86	4115	1538	1353	203	3350	1574	4.03	199.91	12.4	747.2	−66.8	−9.1	−7.52
M9	Wuhai	7.95	25.2	720.8	64	2438	1484	1055	207	1842	1121	3.74	132.37	8.6	579.4	−66.1	−9.2	−5.01
M10	Baotou	8.30	24.4	767.9	68	2777	1448	1131	211	2117	1237	3.48	84.40	9.8	590.2	−65.1	−8.9	−1.90
M11	Baotou	8.22	24.4	774.3	72	2844	1457	1155	210	2107	1257	3.42	146.59	11.8	594.6	−64.9	−9.1	−0.63
M12	Tuoketuo	8.22	23.0	792.4	77	3061	1424	1151	209	2272	1313	3.24	158.54	10.5	599.5	−66.8	−9.2	−0.15
M13	Wupu	8.04	23.4	615.2	70	3233	873	645	397	1193	983	3.32	157.64	28.4	526.5	−97.2	−13.0	−4.71
M14	Hukou	7.74	24.3	696.7	78	2808	1273	1239	364	1745	1161	3.32	166.42	19.9	580.7	−86.1	−11.4	4.49
M15	Qiachuan	8.00	29.0	793.3	92	3288	1441	872	302	2234	1373	3.06	–	18.1	593.9	−71.7	−9.5	−0.35
M16	Tongguan	7.80	29.6	627.8	90	2500	1165	838	441	1369	962	3.34	–	26.3	528.0	−80.8	−11.0	−0.63
M17	Mianchi	7.72	28.2	657.4	90	2576	1229	1351	412	1484	1028	3.88	236.26	29.7	598.7	−79.5	−10.9	2.20
M18	Xiaolangdi	7.65	29.1	663.9	88	2699	1231	939	408	1501	1033	3.48	247.24	27.1	568.6	−79.1	−10.8	−2.30
M19	Xiaolangdi	7.81	29.1	757.8	95	3268	1309	1000	347	1974	1279	3.74	239.56	22.5	635.4	−73.8	−10.0	−6.70
Downstream																		
M20	Huayuankou	7.69	27.6	801.1	92	3122	1413	1065	282	2099	1403	3.66	242.91	19.8	640.8	−68.4	−9.3	−7.74
M21	Gaocun	7.44	26.0	787.8	99	2996	1428	1101	293	2113	1434	3.59	238.94	19.7	640.1	−67.8	−9.2	−8.03
M22	Jinan	7.66	26.9	773.5	101	2934	1408	1080	292	2115	1443	3.41	–	20.3	612.6	−65.4	−8.8	−5.01
M23	Dongying	8.11	24.9	773.9	102	2959	1351	1058	284	2079	1437	2.79	1.91	26.2	569.7	−65.5	−8.7	1.72
Tributaries																		
T1	Huangshui	8.24	19.6	0.5	47	1059	1429	748	213	774	706	3.18	126.95	4.9	425.0	−42.8	−7.0	−0.58
T2	Taohe	8.10	20.8	0.4	42	590	1311	672	182	315	331	3.37	76.69	3.3	359.7	−66.9	−9.8	3.81
T3	Qingshui	8.08	22.6	11440.0	338	85,968	9481	23,100	407	55,586	39,440	4.68	1828.93	54.7	9160.7	−67.5	−8.7	6.93
T4	Wuliangsuhai	9.48	26.8	5989.0	418	43,101	895	8906	47	42,101	6638	6.14	–	52.1	3790.7	−30.5	−1.5	2.54
T5	Kuyehe	8.27	25.0	0.6	64	2763	1131	600	311	916	1240	2.89	85.73	30.4	497.8	−103.8	−13.7	−1.30
T6	Wudinghe	8.13	23.8	0.8	90	3608	1019	1212	378	2017	1022	4.02	–	16.2	619.2	−72.6	−9.0	0.96
T7	Yanhe	7.85	24.5	0.7	85	2915	912	904	350	1650	928	3.26	182.33	31.1	530.4	−96.4	−12.7	−4.70
T8	Fenhe	7.62	28.8	1159.0	261	3668	2648	1508	333	2761	2631	3.18	–	28.4	823.7	−66.7	−8.5	8.51
T9	Weihe	7.79	27.9	617.8	109	2012	1306	747	363	1527	869	3.06	466.25	16.9	519.3	−66.5	−9.6	−8.98
T10	Jinghe	7.82	31.9	932.3	79	5520	1138	1612	422	2996	2063	3.86	312.29	42.2	826.9	−87.0	−11.9	−1.73
T11	Weihe	7.56	29.9	714.8	100	2635	1208	1151	404	1719	1035	3.26	521.05	25.0	582.7	−67.7	−9.6	−1.51
T12	Yiluohe	7.79	31.1	612.4	93	1196	1837	912	235	1166	1016	3.12	–	21.5	485.7	−59.7	−8.1	6.89
T13	Qinghe	7.69	28.60	742.2	60	1148	2394	1110	326	881	1766	3.54	–	15.1	609.1	−67.5	−9.2	3.12
Rain	Baotou	–	–	–	–	–	–	–	–	–	–	–	–	–	–	−113.7	−14.5	–

* NICB (Normalized Inorganic Charge Balance) = (TZ⁺ − TZ⁻)/TZ⁺ × 100%.
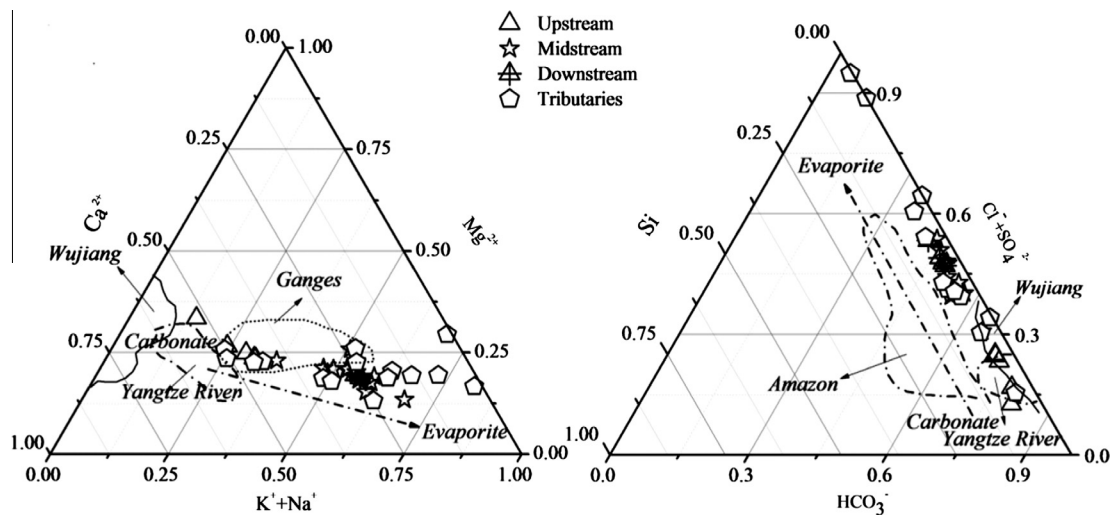

Fig. 2. Ternary diagrams showing compositions of cations (left) and anions (right) in the Huanghe River basin compared with other major river systems. (Data sources: for Yangtze River, Chetelat et al., 2008; for Wujiang River, Han and Liu, 2004; for Amazon River, Gibbs, 1972; and for Ganges River, Sarin et al., 1989).
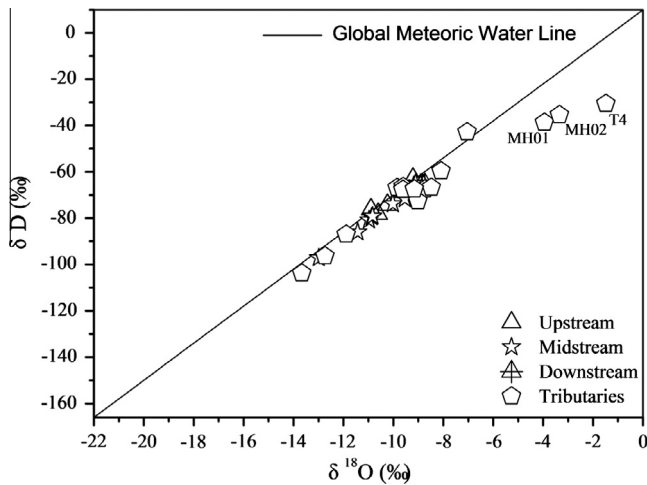
Fig. 3. Plots showing covariations between δD and δ18O of river samples in the Huanghe River basin.

et al., 2003), atmospheric contribution to other elements of the river water were corrected.

The calculated results show that the atmospheric inputs are generally minor in the Huanghe River basin. For the cations, the contribution of atmospheric input range from 0.7% to 2.8% in the upstream, 1.4–7.6% in the midstream, and 4.3–6.7% in the downstream. This finding is consistent with the fact that most of the Huanghe River basin is arid. We also observe that all Huanghe River water samples are enriched in Na and Cl, and composed of the equivalent mole ratios of Na/Cl averaged by 1.54, significantly higher than those of seawater, 0.86 (Zhang et al., 1995), which further demonstrates that the contribution from atmospheric precipitation to the river dissolved load should be expected to be limited.

5.1.2. Anthropogenic influence

It is important to differentiate anthropogenic influences from natural inputs before considering the weathering of different rock types within the river basin. Human activities can greatly influence water chemistry, through waste input and atmospheric input (Flintrop et al., 1996; Xu and Liu, 2007). Variation in total dissolved solutes in river water is not only related to drained basin lithology but also to land use and pollution by human activities (Chetelat et al., 2008; Gaillardet et al., 1999; Han and Liu, 2004). Higher TDS values have been observed in evaporite-influenced rivers, such as the Indus, and in contaminated waters collected in the Changjiang and Wujiang rivers (Chetelat et al., 2008; Han and Liu, 2004; Meybeck, 1987).

In the case of the Huanghe River, the average TDS value, 557 mg/L, is nearly twice that of the Changjiang River (Chetelat et al., 2008), and notably higher than the average TDS value of the world's large rivers (283 mg/L) (Gaillardet et al., 1999). The highest Huanghe River TDS values are observed for sites MH02, T3, and T4. The higher TDS value of site MH02 can be attributed to the influence of evaporite dissolution, given the very low NO3 concentration, and is consistent with the high δ18O value in this region. However, the water chemistry of site T3 has the highest NO3 concentration among all present samples, indicating significant anthropogenic input. A sharp increase in TDS is observed in water samples (sites M7 and M8) in areas of irrigation, indicating the influence of saline irrigation return water. It is evident that intensive agriculture/irrigation activities in the drainage basin, which cycle the leached water back to the river several times, can increase the major ion concentrations (Chen and Wang,

2006). The δ18O in these regions also increase owing to agriculture/irrigation activities that have promoted evaporation.

Nitrate, potassium, chloride and sulfate are commonly considered sensitive to pollution (Flintrop et al., 1996). Additionally, the sulfate and chloride in river waters may have other sources, that is, dissolution of evaporites such as gypsum or halite, or the oxidation of sulfides (Meybeck, 2003; Noh et al., 2009; Ryu et al., 2008). We may link these factors to the TDS variation to decipher the influence of human activities. Polluted water is always characterized by higher Cl/Na and NO3/Na ratios (Gaillardet et al., 1999; Roy et al., 1999), however, as shown in Fig. 4a, all water samples in the Huanghe Rivers show much lower Cl/Na and NO3/Na ratios, with most of the ratios close to the halite end member. In addition, the NO3/K molar ratios in Huanghe River water vary from 0 to 5.4, with most of the samples below 3, lower than the values (around 6) reported for chemical fertilizer in Gansu (Zhang, 2001). The higher values of NO3/K are observed from tributaries (sites T3, T9, T10, and T11) suggesting a significant contribution from anthropogenic inputs. The high concentration of Cl and SO4 but relative lower ratios of SO4/Cl in the rivers, reflect that both gypsum and halite distribute in the basin (Chetelat et al., 2008). The close relationship between Cl and SO4 (Fig. 4b), but lack of correlation between Cl/Na and NO3/Na (Fig. 4a) suggest that Cl and SO4 have similar or the same sources, different from that of NO3, which is most likely of anthropogenic origin.
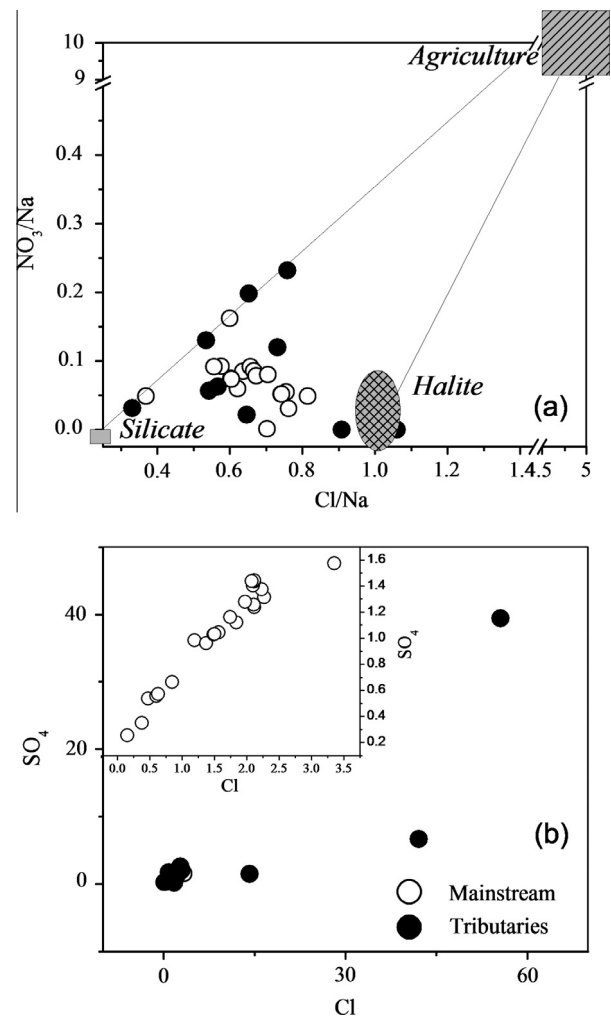

Fig. 4. Plots showing variations of (a) Cl/Na with NO3/Na ratios, and (b) SO4 with Cl. (Data of halite and agriculture end members are from Roy et al. (1999).

The TDS values measured for all water samples, in general, increase with increasing $(Cl + SO_4)/HCO_3$ molar ratios (Fig. 5a), which is obvious for the main channel samples. In contrast, no correlation between TDS and $(NO_3 + Cl)/Na$ is found (Fig. 5b). These observations strongly suggest that contribution from evaporite dissolution overwhelms that from anthropogenic influence, and are supported by the fact that evaporite strata are exposed in the Huanghe River basin (Yokoo et al., 2004; Zhang et al., 1995, 1990a).

The close relationship between K and Na^* indicates that K is mainly sourced from silicate rock weathering, because excess Na, after correction from evaporite and precipitation, is mainly derived from silicate dissolution. The average K/Na^* molar ratio of around 0.1 of the main channel samples is identical to the value reported for silicate draining water (Gaillardet et al., 1999).

The above relationships together indicate that the irrigation return water has a significant influence on river TDS, while the additional contributions of TDS from application of chemical fertilizers and dumping of domestic/industrial wastewater to the solutes is minor.

5.1.3. Identification of rock weathering

Good relationships are observed between Ca/Na versus Mg/Na and Ca/Na versus HCO_3/Na (Fig. 6), similar to data distributions shown by Sr/Na versus Ca/Na. The distribution of the present samples on the figure is highly variable when compared with that of the world's large rivers, but the end members of carbonates, silicates and evaporites can explain all the variability of the water
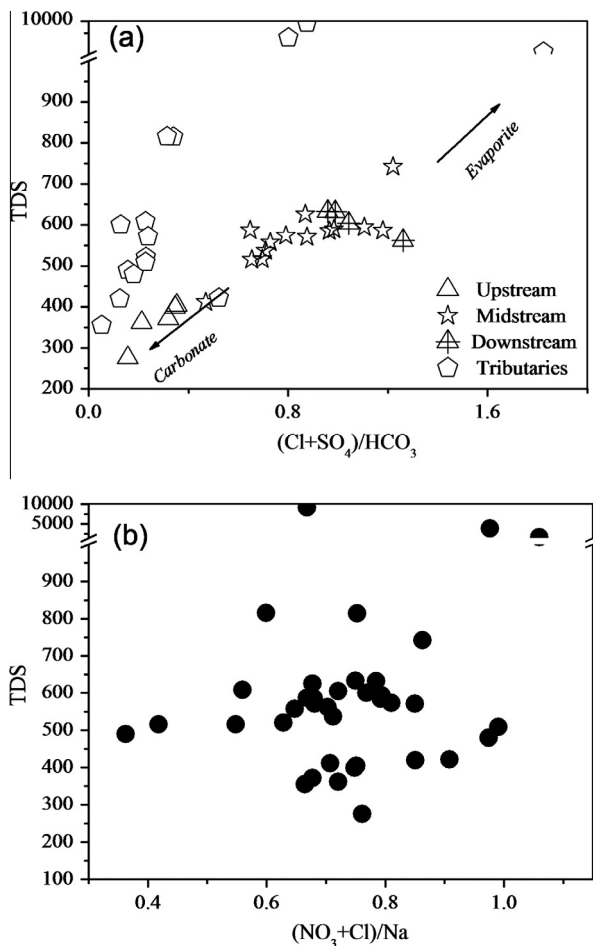

Fig. 5. Plots showing variations of (a) TDS with $(Cl + SO_4)/HCO_3$, and (b) with $(NO_3 + Cl)/Na$, for the Huanghe River main channel from upstream to downstream and its main tributaries.
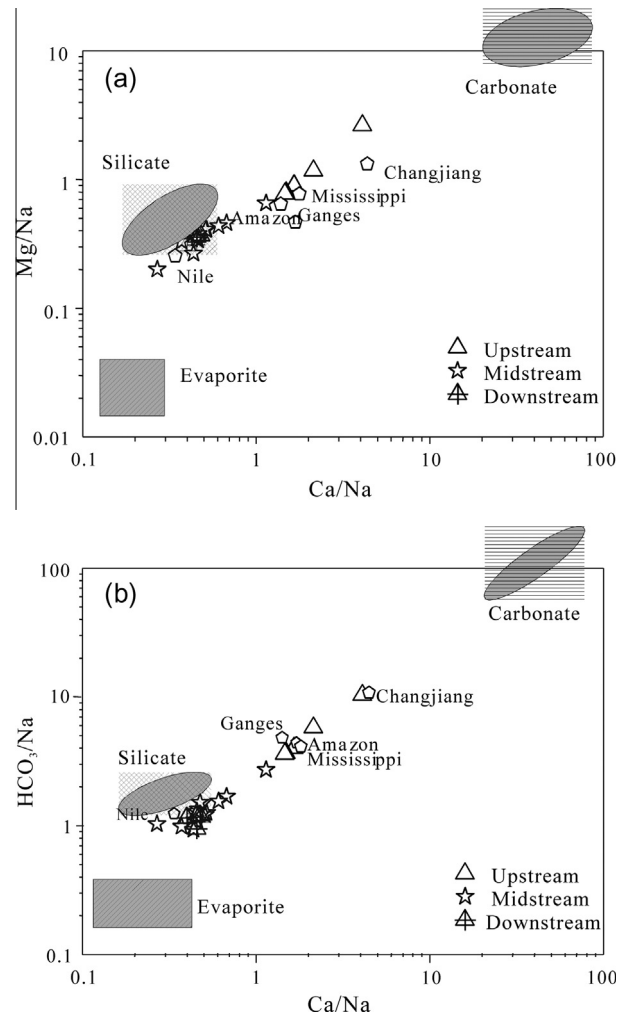

Fig. 6. Plots of (a) Mg/Na vs. Ca/Na and (b) HCO_3/Na vs. Ca/Na for the Huanghe River waters, showing the mixing between carbonate and evaporite end-members. Data from other world rivers, and silicate, carbonate and evaporite end-members are from Gaillardet et al. (1999).

chemical composition. This distribution further suggests that the influence of atmospheric and anthropogenic input is minor. For the Huanghe River main channel, it is worth to note that the Ca/Na, Mg/Na and HCO_3/Na molar ratios of river water samples decrease along the line of carbonate–silicate from the upstream to the downstream and have an obvious downward deviation from the carbonate–silicate line to carbonate–evaporite line.

5.1.3.1. Carbonate weathering.
In many watersheds of the world, carbonate weathering plays an important role in controlling river water chemistry, regardless of which is major rock type or not in local area, because carbonate is more susceptible to weathering than silicate (Karim and Veizer, 2000; Roy et al., 1999). For the Huanghe River, carbonate weathering is also of importance, especially in the upstream segment. As shown in Fig. 2, most of the water samples from upstream locations are Ca–HCO_3 type, aside from the uppermost two samples taken from the headwater. Unlike the upstream, the water samples from the midstream and the downstream are Na–Ca–HCO_3–Cl–SO_4 type. This suggests that carbonate contribution to the river water is buffered by the contribution from evaporite in the midstream, which is in line with the geological evidence of widespread carbonate in the upstream and abundant evaporites in the midstream (Wu et al., 2005; Zhang

et al., 1995, 1990a). In Fig. 6, the data of the upstream samples are close to the carbonate end member, similar to the Changjiang River, indicative of dominance of carbonate weathering. Furthermore, compared with most major rivers in the world, the Huanghe River samples are characterized by higher alkalinity, implying that the contribution from carbonate weathering is significant.

5.1.3.2. Silicate weathering. Silica concentration provides a clear discriminator for distinguishing silicate weathering (Berner et al., 1983; Chetelat et al., 2008; Wu et al., 2005). In the Huanghe River basin, the Si concentration varies from 24 to 213 μM (average 146 μM) in the upstream, from 195 to 441 μM (average 289 μM) in the midstream, and from 282 to 347 μM (average 300 μM) in the downstream waters. Obviously, there is an increasing trend in Si concentration from the upstream to the downstream, which implies that an enhanced silicate weathering occurs toward downstream. Furthermore, from the stoichiometry of these waters, assuming that Cl is balanced only by Na, we show that a considerable amount of Na is balanced by Cl. The remaining Na (Na^*), which is given by subtracting Cl from total Na equivalences, show a good relationship with Si in the Huanghe River main channel. Such relationship would be expected if the Na^* was derived from silicate weathering.

The relationship of $(Na + K)^*/HCO_3$ versus $(Ca + Mg)^*/HCO_3$ ratios is used to differentiate the sources from carbonate weathering and silicate weathering. The $(Na + K)^*$, given by subtracting Cl from total $(Na + K)$ of river samples should account for silicate weathering by carbonic acid; and the $(Ca + Mg)^*$, given by subtracting SO_4 from total $(Ca + Mg)$, represents the amounts of Ca and Mg originated from carbonate or silicate weathering by carbonic acid (Han and Liu, 2004). As shown in Fig. 7, the upstream samples cluster near the cross point of two lines respectively of $(Na + K)^*/HCO_3 = 0$ and $(Ca + Mg)^*/HCO_3 = 1$, whereas the samples taken from the downstream trend away from the cross point, and toward high $(Na + K)^*/HCO_3$ ratio. This result reflects an increasing silicate weathering contribution to the water chemistry from the upstream to the downstream. In Fig. 6, the water samples in the midstream and downstream are close to the silicate end member. Such trends can be interpreted as the promotion of silicate weathering owing to higher temperature and abundant rainfall in the downstream region.

5.1.3.3. Evaporite dissolution. In comparison with other major rivers (Gaillardet et al., 1999), the dominance of Ca, Na, and HCO_3, and significant enrichment in SO_4 and Cl in major ion composition

could be the typical characteristics of the Huanghe River. Chloride plus sulfate account for over 40% of the anions for most of the samples and identify a major contribution from the dissolution of evaporite or soil salts. The dissolution rate of evaporite is 40–80 times higher than granites, and 4–7 times higher than carbonate, according to the estimation of Meybeck (1987), as a consequence, evaporite dissolution can significantly influence the river chemistry even if evaporite outcrops are sparse in the basin.

Previous study have proposed that over 20% of the Huanghe River dissolved load may be contributed by evaporite dissolution (Gaillardet et al., 1999); Wu et al. (2005) also showed that evaporite dissolution plays an important role in the dissolved load of the water samples in the upper Huanghe River, particularly for several headwater tributaries. From Fig. 8, it is evident that the data for most of the Huanghe River waters plotted with slightly downward deviation from the line, $(Ca + Mg):HCO_3^- = 1:2$, and this deviation is more obvious for some tributaries, such as MH02, T3 and T4. The deviation indicates that additional SO_4 is needed to account for the significant excess $Ca + Mg$. The dissolution of sulfate evaporite is a potential source of SO_4, because there is no evidence for presence of pyrite (FeS_2) exposed in the river basin, and the sulfuric acid from precipitation is minor (Larssen et al., 1999). As expected, a good relationship between $Ca + Mg$ and $HCO_3 + SO_4$ is observed, and the strong relationship between $Na + Ca$ and $SO_4 + Cl$ further suggests that evaporites including halite and gypsum exert an important role in Huanghe River chemistry, which is in consistent with previous study (Yokoo et al., 2004).

The high level of TDS is attributed to the evaporite contribution as illustrated in Fig. 5. Halite (NaCl) and gypsum ($CaSO_4 \cdot 2H_2O$) or anhydrite might be the major sources of SO_4 and Cl. In the

Fig. 8. Plots of (a) HCO_3^- vs. $(Mg^{2+} + Ca^{2+})$ and (b) $(HCO_3^- + SO_4^{2-})$ vs. $(Mg^{2+} + Ca^{2+})$ for the Huanghe River waters. Most of the waters require SO_4 to balance.
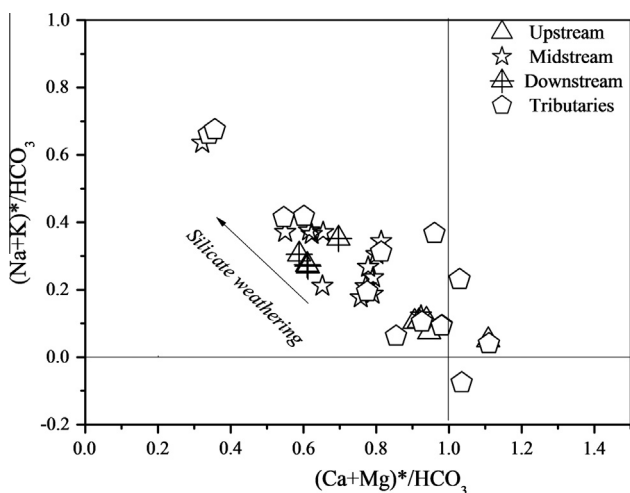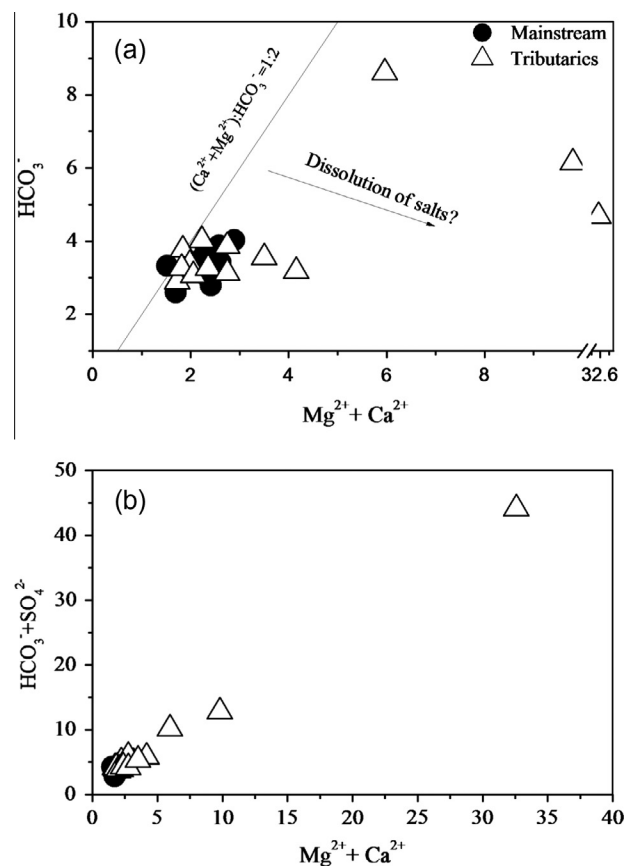

Fig. 7. Relative contributions from silicate and carbonate weathering by carbonic acid for the mainstream samples of the Huanghe River and its main tributaries. For details, see the text.

present study, after the rain correction, we assumed that the SO_4 ($SO_{4evaporite} = SO_{4river} - SO_{4rain}$) and Cl ($Cl_{evaporite} = Cl_{rive} - Cl_{rain}$) in Huanghe River water come from halite and gypsum ($CaSO_4 \cdot 2H_2O$) or anhydrite. The $(Cl + SO_4)$ account for 35% of TZ^- on average, in the upstream, then increasing to 52% in the midstream, 58% in the downstream. These results are in consistent with the increasing trend of Na + Ca, indicating contribution from evaporites dissolution is substantially high in the midstream especially when compared with the upstream.

5.2. Chemical budget and chemical weathering rate estimation

5.2.1. Chemical budget

To quantify the contribution from rain input, evaporite dissolution, carbonate and silicate weathering, a forward model based on mass balance was used in this study. As discussed in Section 5.1.2, assuming negligible contribution from anthropogenic inputs, the forward model is based on mass budget equations for the cations (Na, Ca, Mg, and K) derived from the four possible sources.

Firstly, assuming that the riverine F entirely originate from rainwater, the contribution of atmospheric input is calculated using the cation/F ratios of local rain data (Zhang et al., 2003). After correction of rain contribution, the remaining K ions are assumed to be derived from silicate weathering, and Na is assumed to be derived from silicate weathering as well as evaporite dissolution. The inputs of silicate weathering for riverine Ca and Mg are then estimated using ratios from mono-lithologic streams within the study area. In the present study, we used $(Ca/Na)_{sil} = 0.26$, $(Mg/Na)_{sil} = 0.16$, and $(K/Na)_{sil} = 0.52$ compiled from Wu et al.(2005) and Zhang and Wen (2009).

For each element, we can write mass balance equations with the assumptions discussed above.

$$[F]_{river} = [F]_{atmosphere} \tag{1}$$

$$[Cl]_{river} = [Cl]_{evaporite} + [Cl]_{atmosphere} \tag{2}$$

$$[SO_4]_{river} = [SO_4]_{evaporite} + [SO_4]_{atmosphere} \tag{3}$$

$$[K]_{river} = [K]_{silicate} + [K]_{atmosphere} \tag{4}$$

$$[Na]_{river} = [Na]_{evaporite} + [Na]_{silicate} + [Na]_{atmosphere} \tag{5}$$

$$[Ca]_{river} = [Ca]_{carbonate} + [Ca]_{silicate} + [Ca]_{evaporite} + [Ca]_{atmosphere} \tag{6}$$

$$[Mg]_{river} = [Mg]_{silicate} + [Mg]_{carbonate} + [Mg]_{atmosphere} \tag{7}$$

So the contributions of silicate weathering, carbonate weathering and evaporite dissolution can be calculated using the following equations:

$$\begin{aligned} TDS_{silicate} &= [Na]_{silicate} + [K]_{silicate} + [Ca]_{silicate} + [Mg]_{silicate} \\ &\quad + [SiO_2] \\ &= [Na]_{silicate} + [K]_{silicate} + 0.26 \times [Na]_{silicate} + 0.16 \\ &\quad \times [Na]_{silicate} + [SiO_2]_{silicate} \end{aligned} \tag{8}$$

$$TDS_{carbonate} = [Ca]_{carbonate} + [Mg]_{carbonate} + 1/2HCO_{3carb} \tag{9}$$

$$\begin{aligned} TDS_{evaporite} &= [Na]_{evaporite} + [Ca]_{evaporite} + [Mg]_{evaporite} \\ &\quad + [SO_4]_{evaporite} + [Cl]_{evaporite} \end{aligned} \tag{10}$$

Based on the forward model, 61% of the dissolved loads in the upstream of the Huanghe River come from carbonate weathering, 28% from evaporite dissolution, and only 7% from silicate weathering. In the midstream, 50% of the dissolved loads are sourced from

evaporite dissolution, 34% from carbonates, and only 10% from silicate weathering. Considering the entire Huanghe River basin, dissolved load is originated approximately 56% from evaporite, 28% from carbonate and 12% from silicate. The contributions of evaporite dissolution and silicate weathering increase from the upstream to the downstream, while the contribution of carbonate weathering decreases. Such difference among the three sources can be explained by the variation of lithologic condition along the Huanghe River main channel (Wu et al., 2005; Zhang et al., 1990a), however, increased temperature and rainfall in the downstream would promote silicate weathering as a whole.

Suspended particulate material (SPM) for the Huanghe River water samples were also measured. Results show that the SPM values in the upstream segment are much lower, whereas in the midstream where the river flows through the Loess Plateau, the SPM have an abrupt increase. However, SPM in the downstream show a sharp decrease from the midstream (Table 2), probably influenced by flood control dams (Wang et al., 2006). A slight negative correlation is observed between the TDS and SPM yields in Huanghe River, which may indicate that on one hand flood control dams result in the decrease of SPM, but on the other hand they lead to the increase of ion concentrations because of enhanced evaporation.

5.2.2. Chemical weathering and CO_2 consumption rate

The silicate, carbonate and evaporite weathering rate in the basin can be estimated from our budget of carbonate/silicate/evaporite weathering in combination with hydrological data available on http://www.yellowriver.gov.cn/nishagonggao/2012/index (in Chinese).

The silicate weathering rate is calculated as:

$$\begin{aligned} SWR &= ([Na]_{silicate} + [K]_{silicate} + [Ca]_{silicate} + [Mg]_{silicate} + [SiO_2]) \\ &\quad \times Q \end{aligned} \tag{11}$$

The carbonate weathering rate is calculated as:

$$CWR = ([Ca]_{carbonate} + [Mg]_{carbonate} + 1/2[HCO_3]_{carb}) \times Q. \tag{12}$$

The evaporite dissolution rate is calculated as:

$$\begin{aligned} EWR &= ([Na]_{evaporite} + [Ca]_{evaporite} + [Mg]_{evaporite} + [SO_4]_{evaporite} \\ &\quad + [Cl]_{evaporite}) \times Q. \end{aligned} \tag{13}$$

The rate of CO_2 consumption during silicate and carbonate weathering can be determined from the equation of Moon et al. (2007), as follows:

$$[\Phi CO_2]_{sil} = \Phi(Na_{sil} + K_{sil} + 2Mg_{sil} + 2Ca_{sil}), \tag{14}$$

$$[\Phi CO_2]_{car} = \Phi(Mg_{car} + Ca_{car}), \tag{15}$$

where Φ represents CO_2 consumption rate (mol/km^2/yr) during silicate and carbonate weathering processes. To precisely calculate the chemical weathering and CO_2 consumption rate in the three segments of the river, the water consumption along the Huanghe River basin was considered according to Zhang et al. (2011). The calculated results are shown in Table 2.

5.2.2.1. The role of carbonate, evaporite and silicate weathering in the upstream. The upstream of Huanghe River (samples MH01–M5) has high TDS yield from both carbonate (TDS_{car}, 6.11×10^6 t/yr) and evaporite weathering (TDS_{eva}, 4.64×10^6 t/yr). In comparison, the TDS yield from silicate (TDS_{sil}, 0.52×10^6 t/yr) is significantly lower. The CO_2 consumption rate of silicate weathering is estimated at about 14×10^3 mol/km^2/yr, which is within the range (6–120×10^3 mol/km^2/yr) reported by Wu et al. (2005), but significantly lower than that of carbonate weathering (304×10^3 mol/km^2/yr). Therefore, the upstream of Huanghe River shows dominant carbonate weathering, though clastic rocks are widely distributed in

Table 2
Chemical weathering and CO_2 consumption rate in the mainstream of Huanghe River.

River, location	Surface area (10^4 km^2)	Discharge of outlet (10^9 m^3/yr)	Consumed water (10^9 m^3/yr)	SPM (mg/L)	Silicates			Carbonates			Evaporites	Total rock weathering (10^6 ton/yr)	Total CO_2 consumption (10^9 mol/yr)
					TDS$_{sil}$ (10^6 ton/yr)	ΦCO_2 cons. (10^5 mol/km^2/yr)	CO_2 cons. (10^9 mol/yr)	TDS$_{car}$ (10^6 ton/yr)	ΦCO_2 cons. (10^5 mol/km^2/yr)	CO_2 cons. (10^9 mol/yr)	TDS$_{eva}$ (10^6 ton/yr)		
Upstream	22.3	38.0	2.7	890	0.52	0.14	3.2	6.11	3.04	67.6	4.64	11.3	70.8
Midstream	50.7	38.8	17.0	102,739	0.75	0.21	10.7	1.35	0.65	32.9	13.80	15.9	43.6
Downstream	2.2	28.3	8.7	5136	0.25	5.62	12.3	0.0	0.0	0.0	0.0	0.25	12.3
The whole basin	75.2	28.3	28.7	5136	1.52	0.35	26.2	7.46	1.34	100.5	18.44	27.45	126.7

this region. Two conditions may account for this: (1) abundant carbonates are exposed in the upstream area (Wu et al., 2005; Yang et al., 1986), and (2) carbonates are much more susceptible to chemical weathering than most silicate minerals, particularly under cold conditions like the upstream environment of the Huanghe River.

5.2.2.2. The role of carbonate, evaporite and silicate weathering in the midstream. Compared with the upstream, evaporite dissolution in the midstream is the primary sources of riverine TDS, accounting for 50% of the total Huanghe River TDS yield, while the contribution from both carbonate and silicate weathering is minor. Thus, evaporite dissolution plays an important role in the riverine chemical composition in the midstream, which is consistent with its geological and environmental characteristic. The midstream, mainly the Loess plateau, is dominated by Quaternary loess and loess-like deposits, and evaporites are widely distributed in this region because of the arid climate (Zhang et al., 1995). With respect to CO_2 consumption rate, carbonate weathering is still predominant, accounting for 75% of the total CO_2 consumption rate in the midstream, compared with that of silicate weathering. Higher carbonate weathering is consistent with the fact that loess has a high carbonate content (Zhang et al., 1990b).

5.2.2.3. The role of carbonate, evaporite and silicate weathering in the downstream. According to our calculation, there is no contribution from carbonate and evaporite to the river water chemistry in the downstream location, though a minor contribution from silicate weathering is observed. This observation is consistent with the geological characteristic with Archean to Tertiary granites and metamorphic rocks exposed in the headwater region (Wang et al., 2012; Yang et al., 1986). However, owing to large volume of sediment deposited along the basin, and the few tributaries in this region (Su et al., 2003), both of which have restrained the chemical weathering, the weathering of silicates is not important in affecting river water chemistry in the downstream region. Thus, as shown in Fig. 2, the data points of Huanghe River samples in the midstream and downstream collections nearly overlap. This shows that the chemical compositions in the downstream river water inherit almost completely the features of the upstream and downstream.

Overall, The TDS$_{sil}$ yield of the whole Huanghe River basin is 1.52×10^6 t/yr, similar to the value (2.6×10^6 t/yr) reported by Gaillardet et al. (1999), and the TDS$_{car}$ yield is 7.46×10^6 t/y, while the TDS$_{eva}$ yield (18.44×10^6 t/yr) is much higher. As a whole, we estimate the dissolved load to the ocean carried by the Huanghe River to be 27.45×10^6 t/yr, accounting for 1.3% of the world total flux, and that about 126.7×10^9 mol/yr CO_2 is consumed through reaction with carbonate and silicate rock—which is a little higher than that (109×10^9 mol/yr) reported by Gaillardet et al. (1999) but lower than the value (147×10^9 mol/yr) calculated by Wang et al. (2012).

In general, there is an increasing trend for the CO_2 consumption rate by silicate weathering from 0.14×10^5 mol/km^2/yr in the upstream to 5.62×10^5 mol/km^2/yr in the downstream. However,

the CO_2 consumption rate by carbonate weathering shows an opposite trend, decreasing from 3.04×10^5 mol/km^2/yr in the upstream to near zero in the downstream.

Though we have herein compared our results with prior studies, we note that the calculated results in all studies are not based on the same method, *e.g.*, some researchers used an inverse model, and others used an forward model, or some special parameters were considered, such as the consumed water in this study. Our results may not be directly comparable, and the temporal variation of TDS yield and CO_2 flux should be estimated using the same method and parameters in the future.

6. Conclusions

The Huanghe River displays variable major ion compositions owing to the complex geologic makeup of the drainage basin. In the upstream segment of the Huanghe River above Lanzhou, the water chemistry is controlled by carbonate weathering. In the midstream, where the river traverses through the Loess Plateau, evaporite dissolution is of primary importance in controlling the water chemistry. Downstream near the river mouth, the river inherits the chemical features of the upstream and midstream region, with almost no additional weathering contribution. Weathering contributions from silicate, carbonate and evaporite were estimated by a forward model, which indicate that 56% of the dissolved load came from evaporite, 28% from carbonate and 12% from silicate within the whole basin.

The CO_2 consumption rate by carbonate weathering is highest in the upstream region, 3.04×10^5 mol/km^2/yr, and decline in the downstream region. In contrast, there is an increasing trend in the consumption rate of CO_2 by silicate weathering, from the upstream (0.14×10^5 mol/km^2/yr) to the downstream (5.62×10^5 mol/km^2/yr). In the whole Huanghe River basin, the CO_2 consumption budget is estimated at 126.7×10^9 mol/yr, mostly consumed by carbonate weathering. The chemical weathering rate is 27.5×10^6 t/year, mostly from evaporite dissolution.

References

Berner, R.A., Lasaga, A.C., Garrels, R.M., 1983. The carbonate–silicate geochemical cycle and its effect on atmospheric carbon dioxide over the past 100 million years. Am. J. Sci. 283, 641–683.

Chen, J.S., Wang, F.Y., 2006. Geochemistry of water quality of the Yellow River basin. Earth Sci. Front. 13, 58–73 (in Chinese with English abstract).

Chetelat, B., Liu, C.Q., Zhao, Z.Q., Wang, Q.L., Li, S.L., Li, J., Wang, B.L., 2008. Geochemistry of the dissolved load of the Changjiang Basin rivers: anthropogenic impacts and chemical weathering. Geochim. Cosmochim. Acta 72, 4254–4277.

Chetelat, B., Liu, C.Q., Gaillardet, J., Wang, Q.L., Zhao, Z.Q., Liang, C.S., Xiao, Y.K., 2009. Boron isotopes geochemistry of the Changjiang basin rivers. Geochim. Cosmochim. Acta 73, 6084–6097.

Dessert, C., Dupré, B., Gaillardet, J., François, L.M., Allegre, C.J., 2003. Basalt weathering laws and the impact of basalt weathering on the global carbon cycle. Chem. Geol. 202, 257–273.

Fairchild, I.J., Bradby, L., Sharp, M., Tison, J.L., 1994. Hydrochemistry of carbonate terrains in alpine glacial settings. Earth Surf. Proc. Land. 19, 33–54.

Flintrop, C., Hohlmann, B., Jasper, T., Korte, C., Podlaha, O.G., Scheele, S., Veizer, J., 1996. Anatomy of pollution; rivers of North Rhine-Westphalia, Germany. Am. J. Sci. 296, 58–98.

Gaillardet, J., Dupré, B., Allègre, C.J., 1995. A global geochemical mass budget applied to the Congo Basin rivers: erosion rates and continental crust composition. Geochim. Cosmochim. Acta 59, 3469–3485.

Gaillardet, J., Dupre, B., Allegre, C.J., Négrel, P., 1997. Chemical and physical denudation in the Amazon River Basin. Chem. Geol. 142, 141–173.

Gaillardet, J., Dupré, B., Louvat, P., Allegre, C.J., 1999. Global silicate weathering and CO_2 consumption rates deduced from the chemistry of large rivers. Chem. Geol. 159, 3–30.

Galy, A., Christian, F.L., Louis, A.D., 1999. The strontium isotopic budget of Himalayan rivers in Nepal and Bangladesh. Geochim. Cosmochim. Acta 63, 1905–1925.

Gardner, L.R., Kheoruenromne, I., Chen, H.S., 1981. Geochemistry and mineralogy of an unusual diabase saprolite near Columbia, South Carolina. Clays Clay Miner. 29, 184–190.

Gibbs, R.J., 1972. Water chemistry of the Amazon River. Geochim. Cosmochim. Acta 36, 1061–1066.

Han, G.L., Liu, C.Q., 2004. Water geochemistry controlled by carbonate dissolution: a study of the river waters draining karst-dominated terrain, Guizhou Province, China. Chem. Geol. 204, 1–21.

Huh, Y., Tsoi, M.Y., Zaitsev, A., Edmond, J.M., 1998. The fluvial geochemistry of the rivers of Eastern Siberia: I. Tributaries of the Lena River draining the sedimentary platform of the Siberian Craton. Geochim. Cosmochim. Acta 62, 1657–1676.

Karim, A., Veizer, J., 2000. Weathering processes in the Indus River Basin: implications from riverine carbon, sulfur, oxygen, and strontium isotopes. Chem. Geol. 170, 153–177.

Larssen, T., Seip, H.M., Semb, A., Mulder, J., Muniz, I.P., Vogt, R.D., Lydersen, E., Angell, V., Dagang, T., Eilertsen, O., 1999. Acid deposition and its effects in China: an overview. Environ. Sci. Policy 2, 9–24.

Liu, B.J., Liu, C.Q., Zhang, G., Zhao, Z.Q., Li, S.L., Hu, J., Ding, H., Lang, Y.C., Li, X.D., 2013. Chemical weathering under mid- to cool temperate and monsoon-controlled climate: a study on water geochemistry of the Songhuajiang River system, northeast China. Appl. Geochem. 31, 265–278.

Meybeck, M., 1981. Pathways of major elements from land to ocean through rivers. In: Martin, J.M., Burton, J.D., Eisma, D. (Eds.), River Inputs to the Ocean Systems. UNEP/IOC/SCOR/UNFSCO, Switzerland, pp. 18–30.

Meybeck, M., 1987. Global chemical weathering of surficial rocks estimated from river dissolved loads. Am. J. Sci. 287, 401–428.

Meybeck, M., 2003. Global occurrence of major elements in rivers. Treatise Geochem. 5, 207–224.

Moon, S., Huh, Y., Qin, J., van Pho, N., 2007. Chemical weathering in the Hong (Red) River basin: rates of silicate weathering and their controlling factors. Geochim. Cosmochim. Acta 71, 1411–1430.

Negrel, P., Allègre, C.J., Dupré, B., Lewin, E., 1993. Erosion sources determined by inversion of major and trace element ratios and strontium isotopic ratios in river water: the Congo Basin case. Earth Planet. Sci. Lett. 120, 59–76.

Noh, H., Huh, Y., Qin, J., Ellis, A., 2009. Chemical weathering in the Three Rivers region of Eastern Tibet. Geochim. Cosmochim. Acta 73, 1857–1877.

Raymo, M.E., Ruddiman, W.F., Froelich, P.N., 1988. Influence of late Cenozoic mountain building on ocean geochemical cycles. Geology 16, 649–653.

Roy, S., Gaillardet, J., Allègre, C.J., 1999. Geochemistry of dissolved and suspended loads of the Seine river, France: anthropogenic impact, carbonate and silicate weathering. Geochim. Cosmochim. Acta 63, 1277–1292.

Ryu, J.S., Lee, K.S., Chang, H.W., Shin, H.S., 2008. Chemical weathering of carbonates and silicates in the Han River basin, South Korea. Chem. Geol. 247, 66–80.

Saito, Y., Yang, Z., Hori, K., 2001. The Huanghe (Yellow River) and Changjiang (Yangtze River) deltas: a review on their characteristics, evolution and sediment discharge during the Holocene. Geomorphology 41, 219–231.

Sarin, M.M., Krishnaswami, S., Dilli, K., 1989. Major ion chemistry of the Ganga–Brahmaputra river system: weathering processes and fluxes to the Bay of Bengal. Geochim. Cosmochim. Acta 53, 977–1009.

Stallard, R.F., Edmond, J.M., 1981. Geochemistry of the Amazon: 1. Precipitation chemistry and the marine contribution to the dissolved load at the time of peak discharge.. J. Geophys. Res.: Oceans (1978–2012) 86, 9844–9858.

Su, X.S., Lin, X.Y., Liao, Z.S., Wang, J.S., 2003. Variation of isotopes in the Yellow River along the flow path and its affecting factors. Geochimica 32, 349–357 (in Chinese with English abstract).

Wang, H.J., Yang, Z.S., Saito, Y.S.K., Liu, J.P., Sun, X.X., 2006. Interannual and seasonal variation of the Huanghe (Yellow River) water discharge over the past 50 years: connections to impacts from ENSO events and dams. Global Planet. Change 50, 212–225.

Wang, B., Lee, X.Q., Yuan, H.L., Zhou, H., Cheng, H.G., Cheng, J.Z., Zhou, Z.H., Xing, Y., Fang, B., Zhang, L.K., 2012. Distinct patterns of chemical weathering in the drainage basins of the Huanghe and Xijiang River, China: evidence from chemical and Sr-isotopic compositions. J. Asian Earth Sci. 59, 219–230.

Wu, L.L., Huh, Y., Qin, J., Du, G., van Der Lee, S., 2005. Chemical weathering in the Upper Huang He (Yellow River) draining the eastern Qinghai–Tibet Plateau. Geochim. Cosmochim. Acta 69, 5279–5294.

Xu, Z.F., Liu, C.Q., 2007. Chemical weathering in the upper reaches of Xijiang River draining the Yunnan–Guizhou Plateau, Southwest China. Chem. Geol. 239, 83–95.

Yang, Z.Y., Chang, Y.Q., Wang, H.Z., 1986. The Geology of China. Clarendon Press Oxford.

Yokoo, Y., Nakano, T., Nishikawa, M., Quan, H., 2004. Mineralogical variation of Sr–Nd isotopic and elemental compositions in loess and desert sand from the central Loess Plateau in China as a provenance tracer of wet and dry deposition in the northwestern Pacific. Chem. Geol. 204, 45–62.

Zhang, S., 2001. Characteristics of Nitrogen, Phosphorus and Potassium Nutrient Resources in Farmlands of Gansu. ph.D. Thesis. Lanzhou, Gansu Agriculture University (in Chinese with English abstract).

Zhang, L.J., Wen, Z.C., 2009. Discussion on silicate weathering in the Huanghe drainage basin. Periodical Ocean Univ. China 39, 988–994 (in Chinese with English abstract).

Zhang, J., Huang, W.W., Liu, M.G., Zhou, Q., 1990a. Drainage basin weathering and major element transport of two large Chinese rivers (Huanghe and Changjiang). J. Geophys. Res., 13277–13288.

Zhang, J., Huang, W.W., Shi, M.C., 1990b. Huanghe (Yellow River) and its estuary: sediment origin, transport and deposition. J. Hydrol. 120, 203–223.

Zhang, J., Huang, W.W., Letolle, R., Jusserand, C., 1995. Major element chemistry of the Huanghe (Yellow River), China-weathering processes and chemical fluxes. J. Hydrol. 168, 173–203.

Zhang, D.D., Jim, C.Y., Peart, M.R., Shi, C., 2003. Rapid changes of precipitation pH in Qinghai Province, the northeastern Tibetan Plateau. Sci. Total Environ. 305, 241–248.

Zhang, L.J., Wang, B.S., Xue, M., Wang, L., Wen, Z.C., 2011. Discussion on silicate weathering in the Huanghe Drainage Basin (2): the contribution of water consumption to CO_2 consumption by silicate weathering. Periodical Ocean Univ. China 41, 109–115 (in Chinese with English abstract).